Medipix 2 detector applied to low energy electron microscopy

Gastel, R. van; Sikharulidze, I.; Schramm, S.; Abrahams, J.P.; Poelsema, B.; Tromp, R.M.; Molen, S.J. van der

Ultramicroscopy 110 (2009) 33–35

Contents lists available at ScienceDirect

Ultramicroscopy

journal homepage: www.elsevier.com/locate/ultramic

Medipix 2 detector applied to low energy electron microscopy

R. van Gastel [a,*,1], I. Sikharulidze [b,1], S. Schramm [c], J.P. Abrahams [b], B. Poelsema [a], R.M. Tromp [c,d], S.J. van der Molen [c]

[a] University of Twente, MESA+ Institute for Nanotechnology, P.O. Box 217, NL-7500 AE Enschede, The Netherlands
[b] Leiden University, Leiden Institute of Chemistry, P.O. Box 9502, NL-2300 RA Leiden, The Netherlands
[c] Leiden University, Kamerlingh Onnes Laboratorium, P.O. Box 9504, NL-2300 RA Leiden, The Netherlands
[d] IBM Research Division, T. J. Watson Research Center, P.O. Box 218, Yorktown Heights, NY 10598, USA

ARTICLE INFO

Article history:
Received 25 May 2009
Received in revised form
21 August 2009
Accepted 9 September 2009

PACS:
68.37.Nq
29.40.−n
07.78.+s

Keywords:
Low energy electron microscopy
Photoelectron emission microscopy
Pixel detector

ABSTRACT

Low energy electron microscopy (LEEM) and photo-emission electron microscopy (PEEM) traditionally use microchannel plates (MCPs), a phosphor screen and a CCD-camera to record images and diffraction patterns. In recent years, however, MCPs have become a limiting factor for these types of microscopy. Here, we report on a successful test series using a solid state hybrid pixel detector, Medipix 2, in LEEM and PEEM. Medipix 2 is a background-free detector with an infinite dynamic range, making it very promising for both real-space imaging and spectroscopy. We demonstrate a significant enhancement of both image contrast and resolution, as compared to MCPs. Since aging of the Medipix 2 detector is negligible for the electron energies used in LEEM/PEEM, we expect Medipix to become the detector of choice for a new generation of systems.

1. Introduction

Low energy electron microscopy (LEEM) [1,2] and photo-emission electron microscopy (PEEM) [3] rely on MCPs [4] to convert electrons, backscattered or photo-emitted from a sample, into an image. Since LEEM came to prominence in 1984 [5], MCP units have been the detectors of choice. Unfortunately, the performance of an MCP detector unit is not ideal, so that it has become a limiting factor in the dynamic range of LEEM. A serious drawback is the limited signal intensity that MCPs can handle at their input. Using a 12-bit CCD camera for image recording with MCPs near saturation, a typical image exposure time of 600 ms is needed to utilize the full 12 bit resolution of the imaging system to record a 512×512 pixel image [6]. Unfortunately, frequent overexposure of the MCPs will inevitably lead to beam damage of the MCPs; an effect all too familiar to LEEM operators. Another disadvantage of MCPs are the various sources of noise, such as dark current, thermal noise and the readout noise of the CCD camera used to image the MCPs. The latter is typically the dominant source of noise in LEEM images and constitutes approximately 50 of the available 2^{12} grey levels, depending on the particulars of the camera and its operating parameters. For MCPs the dynamic range is limited by dark counts for very long exposure times ($\geqslant 100$ s). Finally, the spatial resolution of the standard LEEM/PEEM MCP detector is rather modest, with a measured resolution limit of 3.5 linepairs/mm or 140 μm [7,8]. Medipix 2 has the potential of improving on all of these issues [9–11]. It offers a much improved resolution (9 linepairs/mm or 55 μm), a large dynamic range and virtually no background. Furthermore, aging effects were shown to be negligible at the electron energies used in LEEM/PEEM (10–20 keV) [12–14]. In this Letter, we demonstrate that the use of a Medipix 2 detector significantly improves the performance of LEEM and PEEM.

Medipix is a CMOS ASIC chip bump-bonded to a high-resistivity silicon sensor. The sensor consists of an array of 256×256 pixels with 55 μm side lengths. Each pixel operates as a back-biased diode with the p-implanted region near the bump-bond when sufficient bias voltage is applied for full depletion of the silicon sensor. Each individual pixel on the chip contains a signal processing and counting circuit. Background rejection and signal amplification can therefore be performed independently for each pixel by setting a lower and higher threshold. Events are recorded in a 13-bit counter at a maximum rate greater than 100 kHz/pixel.

* Corresponding author.
E-mail address: R.vanGastel@utwente.nl (R. van Gastel).
[1] Both authors contributed equally to this work.

0304-3991/$ - see front matter © 2009 Elsevier B.V. All rights reserved.
doi:10.1016/j.ultramic.2009.09.002

An MCP detector records images at a typical CCD resolution of 512×512 pixels for a 42 mm diameter circular area, and a 12-bit CCD counter. Under practical conditions its maximum count rate is less than 1 kHz/pixel [4]. All in all, Medipix allows for very high count rates, virtually no background, and a superior dynamic range. With the capabilities of LEEM and PEEM extending more and more, particularly into the area of spectroscopic imaging, the requirement for a detector with a large dynamic range and a low background has become urgent.

2. Experimental details

In this study, a single Medipix 2 detector (14×14 mm) was tested in the Elmitec LEEM III instrument at the University of Twente. Measurements were done on an Ir(111) sample with graphene flakes grown on its surface [15]. For this, an Ir(111) sample was first heated to 850 °C and exposed to 1×10^{-7} mbar of O_2 to remove residual carbon contamination. Graphene flakes were subsequently grown at a 5×10^{-8} mbar pressure of ethylene at 900 °C. The growth was stopped when the coverage of graphene was around 40%. PEEM and LEEM images were first recorded using the traditional setup with MCPs and phosphor screen. The detector used was a Chevron model 3040FM MCPs, which had a channel diameter of 10 μm, a 12 μm channel spacing and was operated at a bias voltage of 1350 V. To subsequently test the Medipix detector, the sample chamber was closed and maintained at a vacuum pressure $< 6 \times 10^{-11}$ mbar. Next, the imaging column of the microscope was vented and the MCP detector unit was replaced with a Medipix 2 detector. The entire detector and readout assembly were placed in vacuum on a specially designed adapter flange. The ultimate pressure in the column, after several days of pumping and operating the readout electronics, was 4×10^{-7} mbar with the Medipix assembly switched off and 2×10^{-6} mbar when in operation. The pressure in the sample chamber during Medipix image acquisition was $< 5 \times 10^{-8}$ mbar. Data were retrieved using the 'PixelMan' software [16]. The Medipix chip was positioned 20 mm further down the column relative to the position of the MCPs requiring minor adjustments of the lens system to refocus the image.

3. Results and discussion

In Fig. 1, we compare PEEM and LEEM images taken with both detectors. We note that in PEEM, the Ir appears dark, since its work function (5.3 eV) is higher than the photon energy (4.8 eV). In LEEM the contrast depends on the electron energy at the sample. From the images, it is immediately clear that Medipix 2 yields superior resolution and contrast. This is evidenced by the appearance of a bright line at the edges of the graphene flakes in the Medipix PEEM-image (Fig. 1(b)). For the MCPs, this line is barely visible (Fig. 1(a)). It is also illustrated by the fact that the characteristic 120°- angle at the graphene edge is distinguishable using Medipix (Fig. 1(d)), whereas it is not with the MCPs (it is more rounded in Fig. 1(c)). Recently, it was demonstrated that an equivalent LEEM MCP detector, including the CCD camera, is fundamentally limited to a resolution of 140 μm [7]. For Medipix this number will be 55 μm, provided the electron-hole cloud generated in the detector layer chip does not exceed the size of a pixel. For the relatively low energy electrons in LEEM (10-20 kV), this is indeed the case. To quantify the difference in resolution in our experiments, line scans were taken from the LEEM images of Fig. 1. The position of the line scans is indicated in Fig. 1(c) and (d). It traverses a step, a step bunch and another step, respectively. The step widths on the detector itself (defined from 10 to 90%) for the LEEM images in Fig. 1 are 206, 242 and 140 μm (MCP) and 88, 118 and 84 μm (Medipix 2), respectively. Therefore, the improvement in detector resolution is around a factor of 2, consistent with expectations.

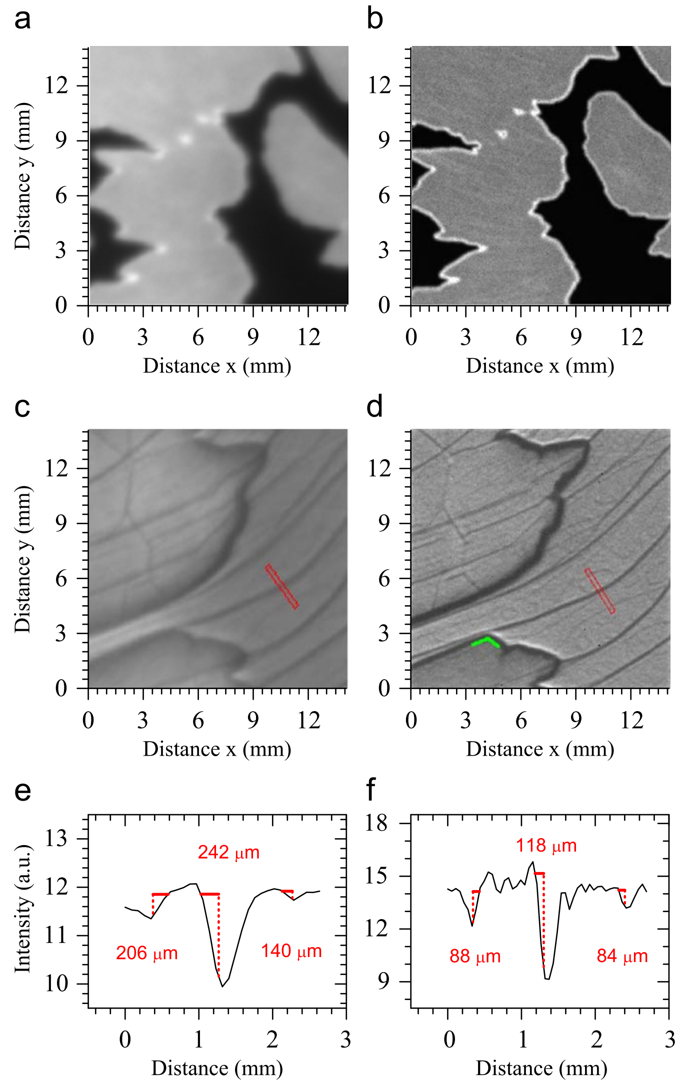

Fig. 1. Comparison of PEEM and LEEM images of graphene flakes on Ir(111), taken with MCP and Medipix 2 detectors at identical magnification and an electron energy of 20 keV. (a) PEEM image with MCP. The dimensions (x, y) relate to the true detector size. The Ir appears dark. (b) PEEM image of same area, taken with Medipix 2. Field of view (FOV) on the sample is 15.5 μm and the image acquisition time is 5 s for both (a) and (b). Note that the full detector area is larger for MCP than for Medipix. Image (a) was therefore cut from a 50 μm FOV MCP image. (c) LEEM image with MCP (FOV: 3.1 μm). (d) The same LEEM image by Medipix 2. The green line indicates a 120° angle at the graphene edge. Both (c) and (d) are averaged over 128 images with an acquisition time of 0.5 s. (e) Line scan from (c). (f) Line scan from (d). (For interpretation of the references to colour in this figure legend, the reader is referred to the web version of this article.)

Medipix 2 was originally designed for the detection of high-energy subatomic particles and photons, so that it is *a priori* unclear how sensitive it is to lower energy electrons [17]. Therefore, we characterized detector count rates in PEEM, for acceleration voltages between 10 kV and 20 kV. At each potential, pixel threshold scans were performed, i.e. we varied the lower threshold value V_{th} of each pixel, while monitoring the number of counts [14]. The resulting scans are plotted in Fig. 2. It illustrates how one can set the lower threshold value for each Medipix pixel, such that optimal count rates are obtained. V_{th} can consequently be converted to an electron threshold energy, E_{th} [14]. For

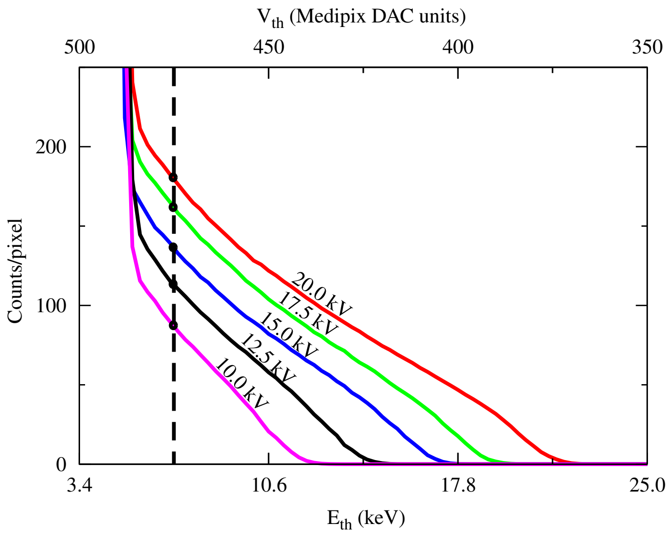

Fig. 2. Lower threshold scans for 5 typical acceleration voltages in PEEM (10–20 kV). For each voltage, the lower pixel threshold value V_{th} was varied and the number of counts monitored. The lower horizontal axis shows the electron energy E_{th} corresponding to a particular V_{th} setting. Numbers adjacent to the lines indicate the actual energy of the incident electrons. We observe an increase in count rate as the acceleration potential is increased. This is illustrated by the line at an electron threshold energy of 7 keV (same sample as in Fig. 1).

decreasing threshold energy E_{th} we observe an increase in counts. For $E_{th} < 5$ keV, the counter registers saturate and images lose their contrast. Therefore, choosing E_{th} somewhat above this value, gives the highest performance. Fig. 2 also shows that the detector count rate increases with the acceleration voltage, as illustrated by the vertical line at $E_{th} = 7$ keV.

One of the promises of Medipix 2 is the possibility to do fast data acquisition. We made movies in LEEM at 20 keV and found that a frame rate of 4.3 per second can be reached with good image quality. For higher frame rates the USB 1.1 interface board [18] used to test the detector becomes the limiting factor. In the near future, a USB 2.0 interface is expected to become available [19]. Thus, we anticipate the exciting possibility of performing LEEM at frame rates above 100 per second.

4. Conclusions

In summary, we have tested a Medipix 2 chip for the detection of electrons with energies up to 20 keV in LEEM/PEEM. We obtain a much better spatial resolution and contrast than for a more conventional, MCP-based detector. Moreover, through appropriate setting of the thresholds, background-free images can be recorded. We expect Medipix to become the standard detector for LEEM and PEEM, because of its many advantages. Clearly, its high resolution and contrast are very beneficial for real space imaging. The possibility of background-free detection with a large dynamic range will give Medipix an edge in spectroscopy as well.

In the near future, the LEEM community is likely to benefit strongly from the impressive activity in the Medipix consortium. First, there are strong efforts to upscale the detector area [21]. The aim is to extend the technique of tiling single chips beyond the already existing 'Quad'-detector. The latter exhibits 2×2 tiling of four single chips, effectively giving a 512×512 pixel detector. Furthermore, fully UHV-compatible detectors are expected to be available before long [20]. Finally, Medipix 3 is coming up [22], with even faster electronics, well-defined counting algorithms and a USB 2.0 interface for high-speed data readout [19].

Acknowledgments

This research was funded by the Netherlands Organization for Scientific Research (NWO) via an NWO-Groot grant ('ESCHER') as well as by the Dutch Foundation for technical sciences (STW). We gratefully acknowledge Ruud van Egmond, Emiel Wiegers and Ewie de Kuyper for technical support. We thank Jan van Ruitenbeek and Wasi Faruqi for inspiring discussions. We are grateful to the CERN and NIKHEF Medipix groups for their advice and support.

References

[1] E. Bauer, Surf. Sci. 102 (1994) 299–300.
[2] R.M. Tromp, IBM J. Res. Dev. 44 (2000) 503.
[3] E. Bauer, J. Electron Spectrosc. 975 (2001) 114–116.
[4] J.L. Wiza, Nucl. Instrum. Methods 162 (1979) 587 (and references therein).
[5] W. Telieps, E. Bauer, Ultramicroscopy 17 (1985) 57.
[6] The camera type used in these experiments is a PCO SensiCam 12 bits CCD camera.
[7] H. Shimizu, T. Yasue, T. Koshikawa, in: Proceedings of the Sixth International Symposium on Atomic Level Characterization for New Materials and Devices ALC '07, Kanazawa, Japan, p. 203.
[8] G. Moldovan, J. Matheson, G. Derbyshire, A. Kirkland, Nucl. Instrum. Methods A 596 (2008) 402.
[9] X. Llopart, M. Campbell, R. Dinapoli, D. San Segundo, E. Pernigotti, IEEE Trans. Nucl. Sci. 49 (2002) 2279.
[10] L. Tlustos, R. Ballabriga, M. Campbell, E. Heijne, K. Kincade, X. Llopart, P. Stejskal, IEEE Trans. Nucl. Sci. 53 (2006) 367.
[11] 〈http://www.cern.ch/medipix/〉.
[12] A.R. Faruqi, Nucl. Instrum. Methods A 466 (2001) 146.
[13] A.R. Faruqi, R. Henderson, L. Tlustos, Nucl. Instrum. Methods A 546 (2005) 160.
[14] G. McMullan, D.M. Cattermole, S. Chen, R. Henderson, X. Llopart, C. Summerfield, L. Tlustos, A.R. Faruqi, Ultramicroscopy 107 (2007) 401.
[15] J. Coraux, A.T. N'Diaye, M. Engler, C. Busse, D. Wall, N. Buckanie, F.J. Meyer-zu-Heringdorf, R. van Gastel, B. Poelsema, T. Michely, New J. Phys. 11 (2009) 023006.
[16] T. Holy, J. Jakubek, S. Pospisil, J. Uher, D. Vavrik, Z. Vykydal, Nucl. Instrum. Methods A 563 (2006) 254.
[17] G. McMullan, S. Chen, R. Henderson, A.R. Faruqi, Ultramicroscopy 109 (2009) 1126.
[18] Z. Vykydal, J. Jakubek, S. Pospisil, Nucl. Instrum. Methods A 563 (2006) 112.
[19] M. Platkevic, V. Bocarov, J. Jakubek, S. Pospisil, V. Tichy, Z. Vykydal, Nucl. Instrum. Methods A 591 (2008) 2454.
[20] J. Visser, J.L. Visschers, private communication.
[21] Z. Vykydal, J. Visschers, D. Sabuncuoglu Tezcan, K. De Munck, T. Borgers, W. Ruythooren, P. De Moor, Nucl. Instrum. Methods A 591 (2008) 241.
[22] R. Ballabriga, M. Campbell, E.H.M. Heijne, X. Llopart, L. Tlustos, IEEE Trans. Nucl. Sci. 54 (2007) 1824.